Tbx15 Defines a Glycolytic Subpopulation and White Adipocyte Heterogeneity

Kevin Y. Lee,[1,2,3] Rita Sharma,[2,3] Grant Gase,[2,3] Siegfried Ussar,[1,4,5] Yichao Li,[6] Lonnie Welch,[6] Darlene E. Berryman,[2,3] Andreas Kispert,[7] Matthias Bluher,[8] and C. Ronald Kahn[1]

Diabetes 2017;66:2822–2829 | https://doi.org/10.2337/db17-0218

Tbx15 **is a member of the T-box gene family of mesodermal developmental genes. We have recently shown that Tbx15 plays a critical role in the formation and metabolic programming of glycolytic myofibers in skeletal muscle.** ***Tbx15*** **is also differentially expressed among white adipose tissue (WAT) in different body depots. In the current study, using three independent methods, we show that even within a single WAT depot, high** ***Tbx15*** **expression is restricted to a subset of preadipocytes and mature white adipocytes. Gene expression and metabolic profiling demonstrate that the Tbx15^{Hi} preadipocyte and adipocyte subpopulations of cells are highly glycolytic, whereas Tbx15^{Low} preadipocytes and adipocytes in the same depot are more oxidative and less glycolytic. Likewise, in humans, expression of** ***TBX15*** **in subcutaneous and visceral WAT is positively correlated with markers of glycolytic metabolism and inversely correlated with obesity. Furthermore, overexpression of Tbx15 is sufficient to reduce oxidative and increase glycolytic metabolism in cultured adipocytes. Thus, Tbx15 differentially regulates oxidative and glycolytic metabolism within subpopulations of white adipocytes and preadipocytes. This leads to a functional heterogeneity of cellular metabolism within WAT that has potential impact in the understanding of human metabolic diseases.**

Over the past decade, it has become clear that adipose tissue and its contribution to metabolic syndrome are more complex than originally believed. Accumulation of visceral white adipose tissue (WAT) is associated with insulin resistance and increased risk of metabolic disease, whereas subcutaneous WAT may be protective against the development of metabolic disorders (1). We and others (2,3) have shown that differences in WAT depots are also marked by differential expression of developmental genes.

Tbx15 is a member of the T-box gene family of developmental genes and has an established role in skeletal formation (4). We have recently shown that in skeletal muscle, Tbx15 is highly and specifically expressed in glycolytic myofibers and regulates the metabolism of these myofibers (5). Furthermore, *Tbx15* is differentially expressed among different WAT depots in both rodents and humans and is markedly downregulated in obesity (2). Genome-wide association studies have shown that a single nucleotide polymorphism near the *TBX15* gene correlates with adiposity in patients of both European and African ancestry (6).

In the current study, we show that even within a single WAT depot, the adipocytes and preadipocytes are heterogeneous with high *Tbx15* expression in only a subset of cells. Metabolic profiling demonstrates that these Tbx15^{Hi} preadipocytes and adipocytes are highly glycolytic, whereas Tbx15^{Low} preadipocytes and adipocytes are more oxidative. Expression of *TBX15* also correlates to markers of glycolytic metabolism in human fat. Finally, we demonstrate that overexpression of Tbx15 is sufficient to drive an increase in glycolytic metabolism in cultured adipocytes. Thus, Tbx15 differentially regulates metabolism in

[1]Section on Integrative Physiology and Metabolism, Joslin Diabetes Center, Harvard Medical School, Boston, MA
[2]Department of Biomedical Sciences, Heritage College of Osteopathic Medicine, Ohio University, Athens, OH
[3]The Diabetes Institute, Ohio University, Athens, OH
[4]JRG Adipocytes and Metabolism, Institute for Diabetes and Obesity, Helmholtz Diabetes Center at Helmholtz Center Munich, Neuherberg, Germany
[5]German Center for Diabetes Research, München-Neuherberg, Germany
[6]Russ College of Engineering and Technology, Ohio University, Athens, OH
[7]Institut für Molekularbiologie, Medizinische Hochschule Hannover, Hannover, Germany
[8]Department of Molecular Endocrinology, University of Leipzig, Leipzig, Germany

Corresponding author: C. Ronald Kahn, c.ronald.kahn@joslin.harvard.edu.

Received 22 February 2017 and accepted 20 August 2017.

This article contains Supplementary Data online at http://diabetes.diabetesjournals.org/lookup/suppl/doi:10.2337/db17-0218/-/DC1.

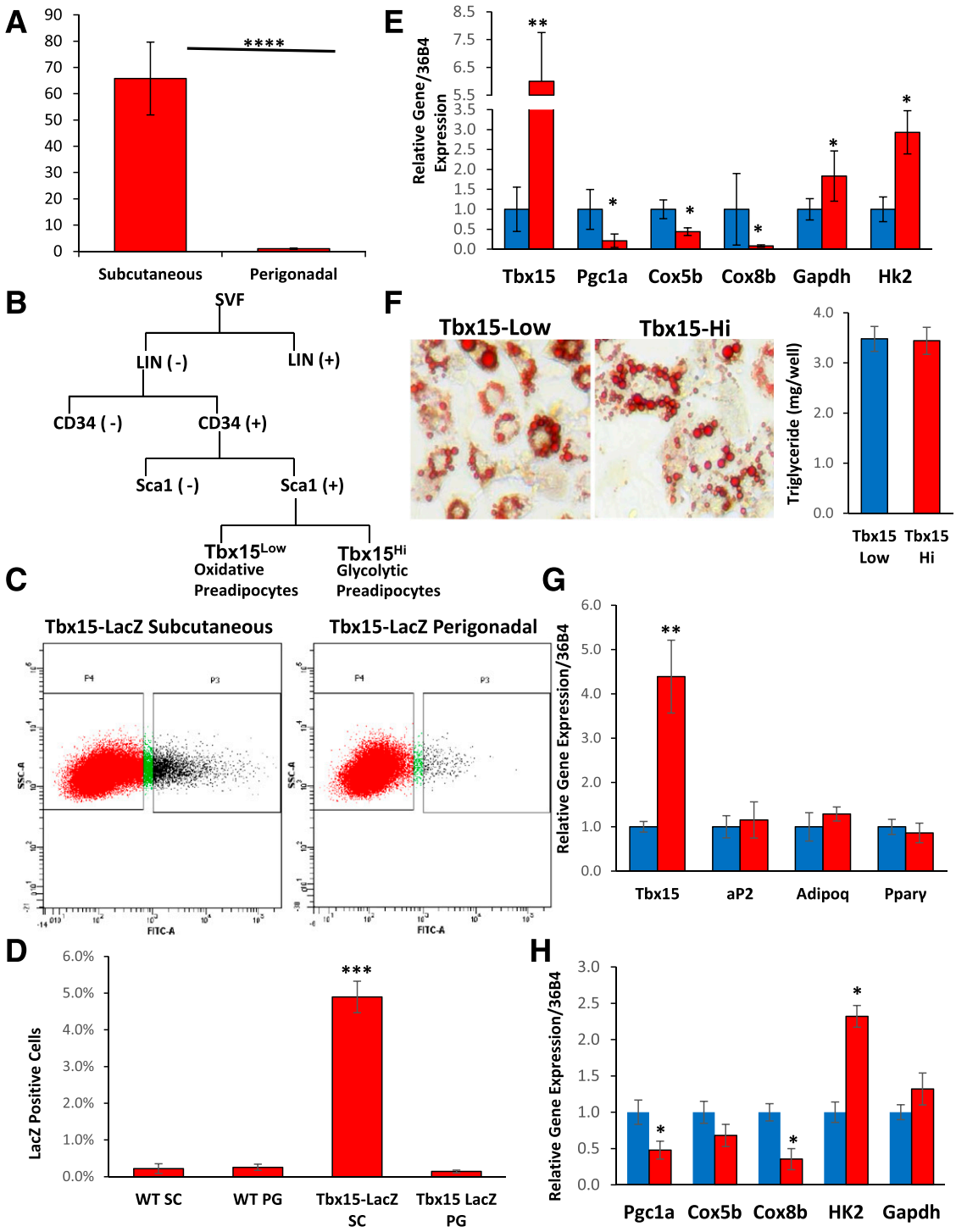

Figure 1—Tbx15 is expressed in a subpopulation of white preadipocytes and is correlated with markers of glycolytic gene expression. Tbx15^{Low} and Tbx15^{Hi} cell lines are shown in blue and red, respectively. *A*: Expression level of *Tbx15* mRNA was compared using qPCR of RNA isolated from subcutaneous and perigonadal fat of 8-week-old male C57BL/6 mice. Data are shown as mean ± SEM of four samples. *B*: Schematic of FACS sorting for Tbx15^{Hi} and Tbx15^{Low} preadipocytes. *C*: Representative FACS plot of LacZ (+) preadipocytes from the subcutaneous and perigonadal fat depots of Tbx15-LacZ male mice at 8–10 weeks of age. *D*: Quantitation of LacZ(+) preadipocytes from WT and Tbx15-LacZ male mice at 8–10 weeks of age. Data are shown as mean ± SEM of three to six animals per group. *E*: qPCR analysis for *Tbx15*, *Pgc1a*, *Cox5b*, *Cox8b*, *Gapdh*, and *Hk2* in RNA isolated from Tbx15^{Hi} and Tbx15^{Low} preadipocytes. Data are shown as mean ± SEM of three to six animals per group. *F*: Oil Red O Staining of Tbx15^{Hi} and Tbx15^{Low} adipocytes after in vitro differentiation. The photographs were taken at ×20 magnification. *G*: qPCR analysis for *Tbx15*, *aP2, Adipoq*, and *Pparγ* in RNA isolated from Tbx15^{Hi} and Tbx15^{Low} adipocytes after in vitro differentiation. Data are shown as mean ± SEM of three to four animals per group. *H*: qPCR analysis for *PGC-1α*, *Cox8b*, Cox5b, *HK2*, and *Gapdh* in RNA samples from *G*. Asterisks indicate significant differences in all panels: *$P < 0.05$; **$P < 0.01$; ***$P < 0.001$; ****$P < 0.0001$. PG, perigonadal; SC, subcutaneous; SVF, stromal vascular fraction; WT, wild type.

white adipocytes and leads to a functional heterogeneity in white fat cells similar to that found among muscle fibers.

RESEARCH DESIGN AND METHODS

Animals and Diets

C57BL/6 mice (The Jackson Laboratory), *Tbx15*-LacZ mice on a mixed genetic background (4), and Immortomouse (7) were housed with a 12-h light/dark cycle in a temperature-controlled room and allowed ad libitum access to water and food (Mouse Diet 9F 5020; PharmaServ). Animal care and study protocols were approved by the Animal Care Committee of Joslin Diabetes Center in accordance with National Institutes of Health guidelines.

Immunofluorescence and In Situ Hybridization

Immunofluorescence using an anti-Tbx15 antibody (8) and fluorescence in situ hybridization (9) were performed as described previously. Regions corresponding to 1,815–2,600 bp of *Tbx15* mRNA and 39–796 bp of *Adipoq* mRNA were cloned into PCRII-TOPO as probe templates. The *Tbx15* probe was labeled by incorporation of uridine-5'-triphosphate–digoxigenin, and the *Adipoq* probe was labeled by incorporation of uridine-5'-triphosphate–biotin. Probes were detected with Alexa Fluor 488 and 594 Tyramine signal amplification kits (Thermo Fisher).

Preadipocyte Isolation, Immortomouse Clonal Cell Lines, and Cell Culture

Preadipocytes were isolated, grown, and differentiated as previously described (10). Preadipocytes were plated, expanded,

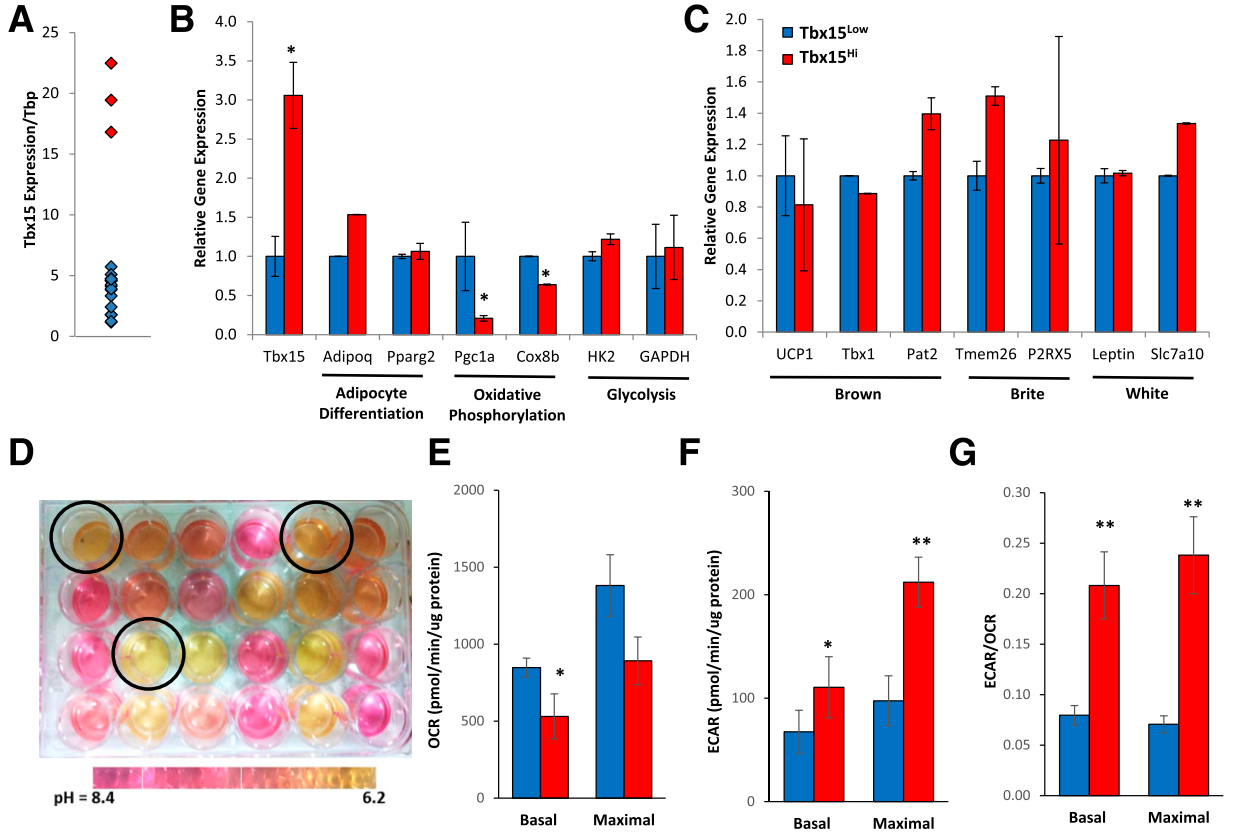

Figure 2—Clonal preadipocyte lines display differences in oxidative and glycolytic metabolism defined by Tbx15 expression. *A*: qPCR analysis for *Tbx15* mRNA in Immortomouse subcutaneous preadipocyte clonal cell lines. Tbx15^{Low} and Tbx15^{Hi} cell lines are shown in blue and red, respectively. *B*: qPCR analysis for *Tbx15* mRNA in Immortomouse preadipocyte clonal cell lines after 4 days of in vitro differentiation. Markers of adipocyte differentiation *Adipoq* and *Pparγ*, markers of oxidative metabolism *Pgc1α* and *Cox8b*, and markers of glycolytic metabolism *HK2* and *Gapdh* were measured. Data are shown as mean ± SEM of 3–15 cell lines per group. *C*: qPCR analysis for *Tbx15* mRNA in Immortomouse clonal preadipocyte cell lines after 4 days of in vitro differentiation. Markers of brown fat *Ucp1*, *Tbx1*, and *Pat2*; markers of brite fat *Tmem26* and *P2RX5*; and markers of white fat *Leptin* and *Slc7a10* were measured. *D*: Representative picture of Immortomouse clonal preadipocyte cell lines and media 48 h after last media change. All wells are 100% confluent, and circled wells indicate Tbx15^{Hi} Immortomouse clonal cell lines. *E*: Basal and maximal respiration of Tbx15^{Low} and Tbx15^{Hi} Immortomouse clonal cell lines after 4 days of in vitro differentiation were determined by calculating the area under the curve during measurements of OCR. Maximal OCR was measured after treatment with 1 μmol/L carbonyl cyanide p-[trifluoromethoxy]-phenyl-hydrazone. The whole experiment was repeated three times. Data are shown as mean ± SEM of 3–15 cell lines per group. *F*: Basal and maximal ECARs of Tbx15^{Low} and Tbx15^{Hi} Immortomouse clonal cell lines after 4 days of in vitro differentiation were determined by calculating the area under the curve during measurements of basal and maximal ECAR. Maximal ECAR was measured after treatment with 1 μmol/L oligomycin. The whole experiment was repeated three times. Data are shown as mean ± SEM of 3–15 cell lines per group. *G*: Ratio of basal and maximal ECAR to OCR of Tbx15^{Low} and Tbx15^{Hi} Immortomouse clonal cell lines after 4 days of in vitro differentiation. Asterisks indicate significant differences in all panels: $^{*}P < 0.05$; $^{**}P < 0.01$.

stained with fluorescein di(β-D-galactopyranoside), and sorted, as previously described (11). Immortomouse clonal lines were created from the subcutaneous fat of a single 8-week-old male mouse. The stromal vascular fraction was isolated, plated, and grown at 33°C in media supplemented with 10 units/mL interferon-γ. A total of 190 individual cells was FACS sorted and grown to clonal cell lines. Twenty of the reproducibly adipogenic cell lines were chosen for further analyses.

Metabolic Analysis

Oxygen consumption rates (OCRs) and extracellular acidification rates (ECARs) were measured using the XF^{e}24 Extracellular Flux Analyzer as previously described (8) using glucose (10 mmol/L), Glutamax (2 mmol/L), and sodium pyruvate (1 mmol/L) as the substrate.

Retroviral and Lentiviral Infection

Tbx15 was stably overexpressed in 3T3-L1 cells using a pBABE-puro retrovirus (8) and knocked down in 3T3-L1 cells by lentiviral short hairpin RNA as previously described (5).

Oil Red O Staining and Triglyceride Quantification

Oil Red O staining and triglyceride quantification were performed as previously described (8).

Human Studies

Gene expression was examined in fat samples obtained from 65 previously described human patients (12). All study protocols have been approved by the Ethics Committee of the University of Leipzig (363–10–13122010 and 017–12–230112).

Statistics

All differences were analyzed by ANOVA or Student *t* test if normally distributed. A Wilcoxon *t* test was used for data that were not normally distributed. Results were considered significant if *P* was <0.05.

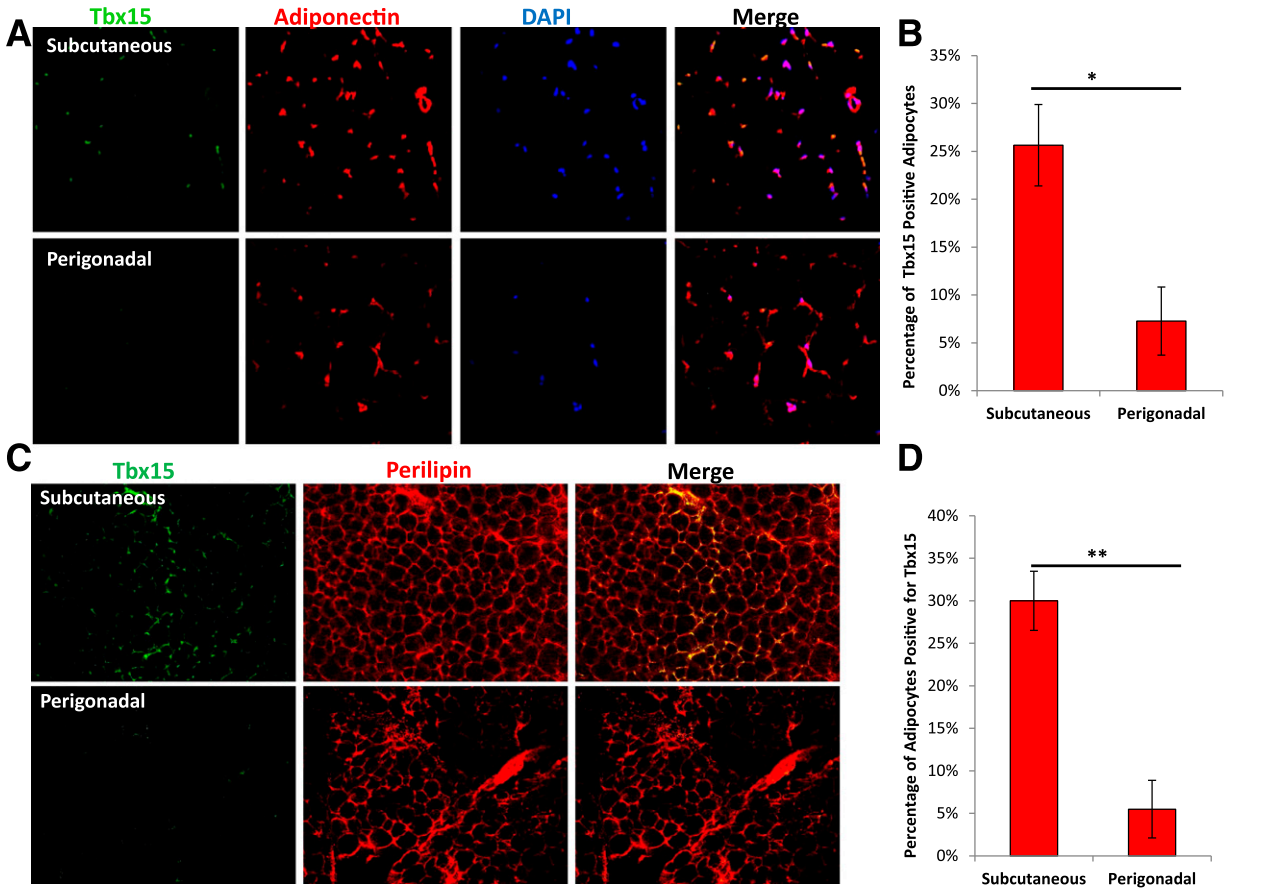

Figure 3—Tbx15 is expressed in a subpopulation of subcutaneous white adipocytes. *A*: Representative images of fluorescence in situ hybridization for *Tbx15* and *Adipoq* in subcutaneous and perigonadal fat of 8-week-old male C57BL/6 mice. Nuclei were counterstained with DAPI. The photographs were taken at ×10 magnification. *B*: Quantitation of *Adipoq*-positive adipocytes that stain positive for *Tbx15* in subcutaneous and perigonadal fat of 8-week-old male C57BL/6 mice as assessed by fluorescence in situ hybridization. Data are shown as mean ± SEM of three animals per group. *C*: Representative images of immunofluorescence for Tbx15 and Perilipin in the subcutaneous fat and perigonadal fat of an 8-week-old C57BL/6 male mouse. Nuclei were counterstained with DAPI. The photographs were taken at ×10 magnification. *D*: Quantitation of Perilipin-positive adipocytes that stain positive for Tbx15 in the subcutaneous fat and perigonadal fat of an 8-week-old C57BL/6 male as assessed by immunofluorescence. Samples were scored by three independent, blinded reviewers. Data are shown as mean ± SEM of three animals per group. Asterisks indicate significant differences in all panels: *$P < 0.05$; **$P < 0.01$.

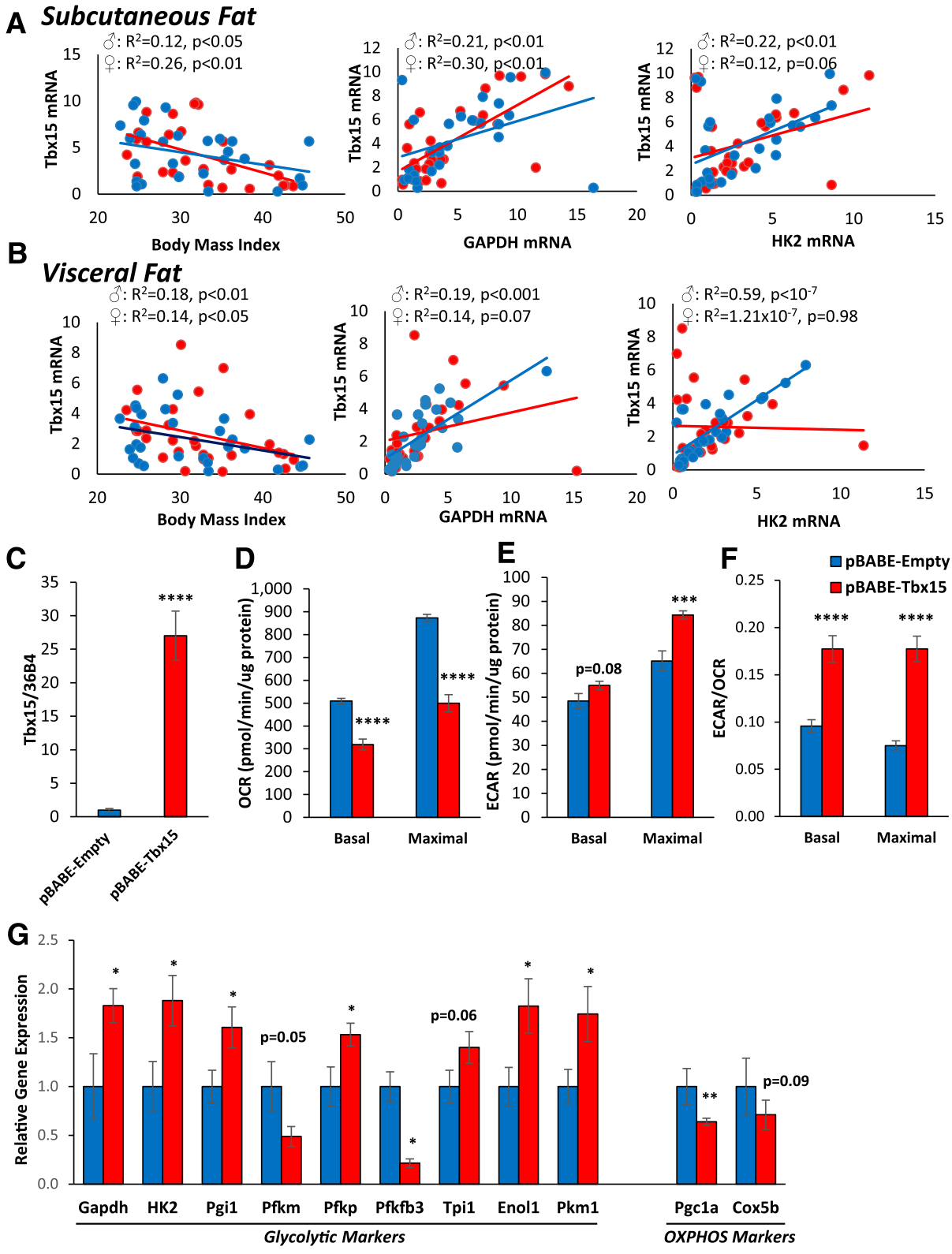

Figure 4—Expression of *TBX15* in human adipose tissue is correlated adiposity and markers of glycolytic metabolism. *A* and *B*: Total of 65 subjects (37 males and 28 females) ranging from lean to obese with variable BMI was subjected to visceral and subcutaneous adipose tissue biopsies. Gene expression of *TBX15*, *HK2*, and *GAPDH* was assessed in both fat depots by qPCR. Blue and red circles represent male and female subjects, respectively. *C*: qPCR analysis for *Tbx15* mRNA was compared between 3T3-L1 cells stably transfected with pBABE-Empty and pBABE-Tbx15 retroviral vectors after adipocyte differentiation. Data are mean ± SEM of six independent samples. *D*: Basal and maximal OCRs of pBABE-Empty and pBABE-Tbx15 3T3-L1 adipocytes was determined by calculating the area under the curve during measurements of OCR. Maximal respiration was measured after treatment of adipocytes with 1 μmol/L carbonyl cyanide p-[trifluoromethoxy]-phenyl-hydrazone. Data are shown as mean ± SEM of 10 cell lines per group, and the experiment was repeated three

RESULTS

We have previously observed that Tbx15 is more highly expressed in subcutaneous than visceral WAT (2) and also much higher in subcutaneous preadipocytes compared with perigonadal preadipocytes (10). Indeed, *Tbx15* mRNA levels were ~60-fold higher in subcutaneous WAT compared with perigonadal WAT of 8-week-old C57BL/6 mice (Fig. 1*A*). To determine if this difference in expression of *Tbx15* among different fat depots was because of an increase of *Tbx15* in all subcutaneous fat cells or to the presence of a subpopulation of cells with high *Tbx15* expression, we FACS sorted preadipocytes isolated from fat pads of *Tbx15*-LacZ reporter mice. Preadipocytes (negative for Ter^{119}, CD45, and CD31 and positive for SCA1 and CD34) (13) were collected and further sorted for *Tbx15* by staining cells with fluorescein di(β-D-galactopyranoside), which is cleaved by β-galactosidase (encoded by the LacZ gene) to release fluorescein isothiocyanate (Fig. 1*B*).

Consistent with the low levels of *Tbx15* in perigonadal fat (2,10), $Tbx15^{Hi}$ preadipocytes were virtually absent in perigonadal fat. By contrast, ~5% of preadipocytes from subcutaneous fat were $Tbx15^{Hi}$ (Fig. 1*C* and *D* and Supplementary Fig. 1*A*). Quantitative real-time PCR (qPCR) analysis of mRNA from these cells confirmed a six-fold higher level in the expression of *Tbx15* compared with $Tbx15^{Low}$ preadipocytes. The $Tbx15^{Hi}$ preadipocytes demonstrated 50–80% lower levels of expression of markers of oxidative metabolism, including *Pgc1a* and cytochrome c oxidase subunits 8b and 5b (*Cox8b* and *Cox5b*). Conversely, $Tbx15^{Hi}$ adipocytes showed 60–120% increases in the markers of glycolytic metabolism hexokinase 2 (*HK2*) and *Gapdh* (Fig. 1*E*). The expression of other markers of oxidative phosphorylation, glycolytic metabolism, and the pentose phosphate pathway was not changed (Supplementary Fig. 1*B*).

Oil Red O staining and quantitation of triglyceride accumulation revealed no morphological differences between $Tbx15^{Hi}$ and $Tbx15^{Low}$ adipocytes after differentiation (Fig. 1*F*). qPCR analysis of differentiated adipocytes confirmed 4.5-fold higher levels of Tbx15 mRNA in $Tbx15^{Hi}$ versus $Tbx15^{Low}$ adipocytes but similar levels of markers of adipogenic differentiation (Fig. 1*G*). However, like the preadipocytes, $Tbx15^{Hi}$ adipocytes had ~30–70% lower levels of oxidative metabolism markers *Pgc1a*, *Cox5b*, and *Cox8b* and ~20–140% higher levels of the glycolytic metabolism markers *HK2* and *Gapdh* (Fig. 1*H*). Furthermore, $Tbx15^{Hi}$ adipocytes had a trend toward decreasing markers of brown/brite fat compared with $Tbx15^{Low}$ adipocytes (Supplementary Fig. 1*C*). Thus, Tbx15 expression marks a distinct subpopulation of preadipocytes and white adipocytes with high expression of markers of glycolytic metabolism and low expression of markers of oxidative metabolism.

To further investigate how heterogeneity in Tbx15 expression affects the adipocyte biology, we isolated single preadipocytes by FACS and created conditionally immortalized clonal adipogenic cell lines from the WAT of an Immortomouse (7). qPCR analysis demonstrated that 17 of these clonal cell lines had relatively low expression of *Tbx15* mRNA ($Tbx15^{Low}$), whereas 3 of these cell lines had expression levels approximately five-fold higher ($Tbx15^{Hi}$) (Fig. 2*A*). This higher level of *Tbx15* persisted after adipogenic differentiation, whereas lipid accumulation and the expression of markers of differentiation were unchanged (Fig. 2*B*). However, like the primary adipocytes, these $Tbx15^{Hi}$ adipocytes had ~70% lower expression of *Pgc1a* and ~30% reduction in *Cox8b* compared with $Tbx15^{Low}$ adipocytes. In contrast, in these immortalized cells, there were no differences in the expression of glycolytic enzymes or expression for markers of brown, brite, or white fat (14) (Fig. 2*B* and *C*).

During culture of these clonal cell lines, we observed differences in media acidification (ranging from pH 8.4 to 6.2) visualized by the color of the media (Fig. 2*D*). Lactic acid production, an end product of glycolysis, contributes to media acidification (15). The highly glycolytic $Tbx15^{Hi}$ cell lines (circled wells) all demonstrated high media acidification rates with an average pH of 6.4, whereas the $Tbx15^{Low}$ cells exhibited a mixture of high and low acidification rates and had an average pH of 7.2. Seahorse flux analysis confirmed these metabolic differences with a 35–40% reduction in basal and maximal OCRs and 50–65% higher basal and maximal ECARs in $Tbx15^{Hi}$ versus $Tbx15^{Low}$ preadipocytes (Fig. 2*E* and *F*). This resulted in an approximately three-fold increase in the ratio of ECAR/OCR in $Tbx15^{Hi}$ cells, indicating a shift from oxidative to glycolytic metabolism (Fig. 2*G*). Treatment with known inducers of thermogenic markers in brite adipocytes, including treatment with 3.3 nmol/L BMP7 for 3 days prior to differentiation (16) and acute treatment with 10 μmol forskolin for 4 h (17), resulted in no differences in *Ucp1* expression between $Tbx15^{Hi}$ and $Tbx15^{Low}$ adipocytes. Although forskolin treatment was able to markedly upregulate *Ucp1* expression in both $Tbx15^{Hi}$ and $Tbx15^{Low}$ adipocytes, expression levels of *Ucp1* in these cells remained 50-fold lower than those observed in brown adipocytes (Supplementary Fig. 2).

times. *E*: Basal and maximal ECAR of pBABE-Empty and pBABE-Tbx15 adipocytes was determined by calculating the area under the curve during measurements of basal and maximal ECAR. Maximal ECAR was measured after treatment of adipocytes with 1 μmol/L oligomycin. The whole experiment was repeated three times. Data are shown as mean ± SEM of 10 cell lines per group, and the experiment was repeated three times. *F*: Ratio of basal and maximal ECAR to OCR of pBABE-Empty and pBABE-Tbx15 adipocytes after in vitro differentiation. *G*: qPCR analysis for *Gapdh*; *HK2*; glucose-6-phosphate isomerase (*Pgi1*); phosphofructokinase, muscle (*Pfkm*); phosphofructokinase, platelet (*Pfkp*); 6-phosphofructo-2-kinase/fructose-2,6-biphosphatase 3 (*Pfkb3*); triosephosphate isomerase (*Tpi1*); enolase (*Enol1*); pyruvate kinase1 (*Pkm1*); *Pgc1a*; and *Cox5b* in RNA isolated from pBABE-Empty and pBABE-Tbx15 adipocytes after in vitro differentiation. Data are shown as mean ± SEM of six independent samples. Asterisks indicate significant differences in all panels: $^{*}P < 0.05$; $^{**}P < 0.01$; $^{***}P < 0.001$; $^{****}P < 10^{-4}$.

Heterogeneity of Tbx15 expression in white adipocytes was also observed in vivo. Compared with adiponectin expression, a marker of all mature white adipocytes, fluorescence in situ hybridization demonstrated that *Tbx15* could be detected in only ~25% of mature adipocytes in subcutaneous WAT and was virtually absent in adipocytes in perigonadal WAT (Fig. 3*A* and *B*). Similarly, immunofluorescence demonstrated that Tbx15 protein was not uniformly expressed, but was expressed in ~30% of subcutaneous adipocytes and in only ~7% perigonadal adipocytes (Fig. 3*C* and *D*). Although Tbx15 is expressed in preadipocytes, >95% of Tbx15-positive cells were also positive for adiponectin, presumably reflecting higher numbers of adipocytes to preadipocytes in the mature fat pad. These results correlate with the differential Tbx15 expression between these depots and demonstrate that Tbx15 expression defines adipocyte subpopulations within a single fat depot.

In human adipose tissue, *TBX15* mRNA expression in adipose tissue was negatively correlated with BMI in both males and females. This was true of mRNA expression from both subcutaneous fat and visceral fat. Furthermore, *TBX15* expression was significantly correlated with *GAPDH* and *HK2* expression in both the visceral and subcutaneous WAT of males, with similar trends found in the subcutaneous WAT of females (Fig. 4*A* and *B*). To more directly investigate if Tbx15 directly regulates oxidative and glycolytic metabolism, we used a pBABE retrovirus to stably overexpress Tbx15 in a 3T3-L1 cell line, pBABE-Tbx15. These cells had a 25-fold overexpression of Tbx15 at the mRNA level (Fig. 4*C*). As we have previously reported (18), Seahorse flux analysis confirmed pBABE-Tbx15 cells had a 40–45% reduction in basal and maximal OCRs (Fig. 4*D*). pBABE-Tbx15 cells also have a 30% higher maximal ECAR that was fully suppressed by addition of 2-deoxyglucose (Fig. 4*E* and Supplementary Fig. 3*A* and *B*). These changes led to an approximately two-fold increase in the ratio of ECAR/OCR in pBABE-Tbx15 cells, indicating a shift from oxidative to glycolytic metabolism (Fig. 4*F*), as well as the change in the expression of enzymes that regulate glycolysis and oxidative phosphorylation (Fig. 4*G* and Supplementary Fig. 3*C*). In contrast, stable lentiviral reduction of Tbx15 in 3T3-L1 cells (shTbx15 cells) did not lead to observable changes in triglyceride accumulation, adipocyte differentiation, ECAR, OCR, or the expression of regulators of oxidative phosphorylation and glycolysis (Supplementary Fig. 3*D*–*I*).

DISCUSSION

In the current study, we have used three independent methodologies—FACS analysis, clonal cell lines, and histology—to demonstrate that Tbx15 is a marker of white adipocytes and preadipocyte heterogeneity that marks a highly glycolytic subpopulation of cells. These data closely parallel our previous finding that Tbx15 is expressed specifically in glycolytic skeletal muscle fibers. We also find that *TBX15* levels in WAT of human subjects are negatively correlated with BMI and positively correlated with markers of glycolytic metabolism (Fig. 4*A* and *B*) (2,19). Taken together, these data strongly suggest that reduced *TBX15* expression in obesity may be, at least in part, because of reduced numbers of highly glycolytic $Tbx15^{Hi}$ cells. Thus, obesity leads not only to adipocyte hypertrophy and hyperplasia, but also to a shift in the cellular composition of the WAT.

We have previously shown in 3T3-L1 cells that overexpression of Tbx15 negatively regulates oxidative metabolism by reducing mitochondrial mass and activity (Fig. 4*D*) (18). In this article, we extend these studies to demonstrate that the reduced oxidative capacity of these cells is accompanied by an increase in glycolytic capacity. Thus, the increased glycolytic metabolism associated with high Tbx15 expression observed in primary adipocytes may be an adaptive response to compensate for reduced oxidative capacity. Indeed, obesity is correlated with both mitochondrial dysfunction (20) and increased basal lactate release (21), although the contribution of Tbx15 to these effects is not yet clear.

Although much attention has been paid to identifying differences between white, brown, and beige adipocytes, recent studies begun to show further molecular intradepot heterogeneity within these classifications (22–24). These studies serve to complement to earlier studies that demonstrate the functional heterogeneity of adipocytes in processes including glucose uptake (25), lipogenesis (26), lipolysis (27), and free fatty acid uptake (28). Importantly, although some cell-culture models have suggested that Tbx15 might be a marker of brite fat (29), we find that even after induction with BMP7 and forskolin that $Tbx15^{Hi}$ white adipocytes tend to have reduced expression of brown/brite fat markers compared with the $Tbx15^{Low}$ adipocytes.

In summary, our results show that the differential expression of Tbx15 leads to metabolic heterogeneity of white preadipocyte and adipocytes, even within a single depot. In both mice and, to some extent, humans, these $Tbx15^{Hi}$ cells display lower oxidative and higher glycolytic metabolism than $Tbx15^{Low}$ cells. Thus, just as we consider muscle fiber type when investigating muscle metabolism, it will be necessary to consider fat cell subtype when investigating adipocyte metabolism. Further investigation of these adipocyte subpopulations and the specific role of glycolytic and oxidative adipocytes in adipose tissue will potentially provide new targets in the treatment of obesity and its related disorders.

Acknowledgments. The authors thank Christie Penniman (Joslin Diabetes Center) for animal care, Jonathan Dreyfuss (Joslin Diabetes Center) for statistical analysis, Girijesh Buruzula and Joyce LaVecchio (Diabetes Research Center Flow Cytometry Core, Joslin Diabetes Center), Michele Pate (Ohio University Flow Cytometry Core), Misako Hata (Edison Biotechnical Institute, Ohio University), and Chris Cahill (Diabetes Research Center Microscopy Core, Joslin Diabetes Center) for technical assistance.

Funding. This work was supported by National Institutes of Health Grant R01-DK-082655 (to C.R.K.), a Research Center Grant P30-DK-036836 (to Joslin Diabetes Center), and a Training Grant T32-DK-007260 (to Joslin Diabetes Center); an American Diabetes Association mentor-based award (to C.R.K.); the Mary K. Iacocca Professorship (to C.R.K.); start-up funds from Ohio University College of Osteopathic Medicine (to K.Y.L.); American Diabetes Association Junior Faculty Development Award 1-17-JDF-055 (to K.Y.L.); and German Research Council Grant DFG KI728/3 (to A.K.).

Duality of Interest. No potential conflicts of interest relevant to this article were reported.

Author Contributions. K.Y.L. designed and performed experiments, analyzed data, and wrote the paper. R.S., G.G., S.U., and M.B. designed and performed experiments. Y.L. and L.W. analyzed data. D.E.B. and A.K. designed experiments and analyzed data. C.R.K. designed experiments, analyzed data, and wrote the paper. All authors discussed the results and implications and commented on the manuscript at all stages. C.R.K. is the guarantor of this work and, as such, had full access to all of the data in the study and takes responsibility for the integrity of the data and the accuracy of the data analysis.

References

1. Tran TT, Yamamoto Y, Gesta S, Kahn CR. Beneficial effects of subcutaneous fat transplantation on metabolism. Cell Metab 2008;7:410–420
2. Gesta S, Blüher M, Yamamoto Y, et al. Evidence for a role of developmental genes in the origin of obesity and body fat distribution. Proc Natl Acad Sci U S A 2006;103:6676–6681
3. Tchkonia T, Lenburg M, Thomou T, et al. Identification of depot-specific human fat cell progenitors through distinct expression profiles and developmental gene patterns. Am J Physiol Endocrinol Metab 2007;292:E298–E307
4. Singh MK, Petry M, Haenig B, Lescher B, Leitges M, Kispert A. The T-box transcription factor Tbx15 is required for skeletal development. Mech Dev 2005;122: 131–144
5. Lee KY, Singh MK, Ussar S, et al. Tbx15 controls skeletal muscle fibre-type determination and muscle metabolism. Nat Commun 2015;6:8054
6. Yoneyama S, Yao J, Guo X, et al. Generalization and fine mapping of European ancestry-based central adiposity variants in African ancestry populations. Int J Obes 2017;41:324–331
7. Jat PS, Noble MD, Ataliotis P, et al. Direct derivation of conditionally immortal cell lines from an H-2Kb-tsA58 transgenic mouse. Proc Natl Acad Sci U S A 1991;88: 5096–5100
8. Lee KY, Gesta S, Boucher J, Wang XL, Kahn CR. The differential role of Hif1β/Arnt and the hypoxic response in adipose function, fibrosis, and inflammation. Cell Metab 2011;14:491–503
9. Pinaud R, Mello CV, Velho TA, Wynne RD, Tremere LA. Detection of two mRNA species at single-cell resolution by double-fluorescence in situ hybridization. Nat Protoc 2008;3:1370–1379
10. Macotela Y, Emanuelli B, Mori MA, et al. Intrinsic differences in adipocyte precursor cells from different white fat depots. Diabetes 2012;61:1691–1699
11. Guo W, Wu H. Detection of LacZ expression by FACS-Gal analysis [article online], 2008. Available at https://www.nature.com/protocolexchange/protocols/446. Accessed 27 August 2017
12. Klöting N, Fasshauer M, Dietrich A, et al. Insulin-sensitive obesity. Am J Physiol Endocrinol Metab 2010;299:E506–E515
13. Rodeheffer MS, Birsoy K, Friedman JM. Identification of white adipocyte progenitor cells in vivo. Cell 2008;135:240–249
14. Ussar S, Lee KY, Dankel SN, et al. ASC-1, PAT2, and P2RX5 are cell surface markers for white, beige, and brown adipocytes. Sci Transl Med 2014;6:247ra103
15. Montcourrier P, Silver I, Farnoud R, Bird I, Rochefort H. Breast cancer cells have a high capacity to acidify extracellular milieu by a dual mechanism. Clin Exp Metastasis 1997;15:382–392
16. Tseng YH, Kokkotou E, Schulz TJ, et al. New role of bone morphogenetic protein 7 in brown adipogenesis and energy expenditure. Nature 2008;454: 1000–1004
17. Wu J, Boström P, Sparks LM, et al. Beige adipocytes are a distinct type of thermogenic fat cell in mouse and human. Cell 2012;150:366–376
18. Gesta S, Bezy O, Mori MA, Macotela Y, Lee KY, Kahn CR. Mesodermal developmental gene Tbx15 impairs adipocyte differentiation and mitochondrial respiration. Proc Natl Acad Sci U S A 2011;108:2771–2776
19. Schleinitz D, Klöting N, Lindgren CM, et al. Fat depot-specific mRNA expression of novel loci associated with waist-hip ratio. Int J Obes 2014;38:120–125
20. Kusminski CM, Scherer PE. Mitochondrial dysfunction in white adipose tissue. Trends Endocrinol Metab 2012;23:435–443
21. DiGirolamo M, Newby FD, Lovejoy J. Lactate production in adipose tissue: a regulated function with extra-adipose implications. FASEB J 1992;6: 2405–2412
22. Sanchez-Gurmaches J, Guertin DA. Adipocytes arise from multiple lineages that are heterogeneously and dynamically distributed. Nat Commun 2014; 5:4099
23. Lee YH, Kim SN, Kwon HJ, Granneman JG. Metabolic heterogeneity of activated beige/brite adipocytes in inguinal adipose tissue. Sci Rep 2017;7:39794
24. Xue R, Lynes MD, Dreyfuss JM, et al. Clonal analyses and gene profiling identify genetic biomarkers of the thermogenic potential of human brown and white preadipocytes. Nat Med 2015;21:760–768
25. Salans LB, Dougherty JW. The effect of insulin upon glucose metabolism by adipose cells of different size. Influence of cell lipid and protein content, age, and nutritional state. J Clin Invest 1971;50:1399–1410
26. Gliemann J, Vinten J. Lipogenesis and insulin sensitivity of single fat cells. J Physiol 1974;236:499–516
27. Seydoux J, Muzzin P, Moinat M, Pralong W, Girardier L, Giacobino JP. Adrenoceptor heterogeneity in human white adipocytes differentiated in culture as assessed by cytosolic free calcium measurements. Cell Signal 1996;8:117–122
28. Varlamov O, Chu M, Cornea A, Sampath H, Roberts CT Jr. Cell-autonomous heterogeneity of nutrient uptake in white adipose tissue of rhesus macaques. Endocrinology 2015;156:80–89
29. Gburcik V, Cawthorn WP, Nedergaard J, Timmons JA, Cannon B. An essential role for Tbx15 in the differentiation of brown and "brite" but not white adipocytes. Am J Physiol Endocrinol Metab 2012;303:E1053–E1060